Arthritis Research & Therapy

https://doi.org/10.1186/s13075-026-03819-5

Article in Press

Revisiting osteoarthritis as an inflammatory disease: characterization of synovitis grading and synovial pathotypes in surgical specimens

Received: 2 March 2026

Accepted: 19 April 2026

Published online: 28 April 2026

Cite this article as: Ciaffi J., Bianchi L., Gambarotti M. *et al.* Revisiting osteoarthritis as an inflammatory disease: characterization of synovitis grading and synovial pathotypes in surgical specimens. *Arthritis Res Ther* (2026). https://doi.org/10.1186/s13075-026-03819-5

Jacopo Ciaffi, Lorenzo Bianchi, Marco Gambarotti, Alberto Righi, Dilia Giuggioli, Roberto Caporali, Cesare Faldini, Stefano Zaffagnini, Tom W. J. Huizinga & Francesco Ursini

Revisiting osteoarthritis as an inflammatory disease: characterization of synovitis grading and synovial pathotypes in surgical specimens

Jacopo Ciaffi [1,2 *†], Lorenzo Bianchi [3,4 †], Marco Gambarotti [5], Alberto Righi [5], Dilia Giuggioli [3,4], Roberto Caporali [6, 7], Cesare Faldini [2,8], Stefano Zaffagnini [2,9], Tom W J Huizinga [10], Francesco Ursini [1,2]

[1] Medicine & Rheumatology Unit, IRCCS Istituto Ortopedico Rizzoli, Bologna, Italy.

[2] Department of Biomedical and Neuromotor Sciences (DIBINEM), Alma Mater Studiorum University of Bologna, Bologna, Italy.

[3] Rheumatology Unit, Azienda Ospedaliero-Universitaria Policlinico di Modena, University of Modena and Reggio Emilia, Modena, Italy.

[4] Department of Medical and Surgical Sciences for Children and Adults, University of Modena and Reggio Emilia, Modena, Italy.

[5] Department of Pathology, IRCCS Istituto Ortopedico Rizzoli, Bologna, Italy.

[6] Department of Clinical Sciences and Community Health, University of Milan, Milan, Italy.

[7] Department of Rheumatology and Medical Sciences, ASST Pini-CTO, Milan, Italy.

[8] 1st Orthopaedic and Traumatologic Clinic, IRCCS Istituto Ortopedico Rizzoli, Bologna, Italy.

[9] 2nd Orthopaedic and Traumatologic Clinic, IRCCS Istituto Ortopedico Rizzoli, Bologna, Italy.

[10] Department of Rheumatology, Leiden University Medical Center, Leiden, the Netherlands.

* Correspondence: Dr. Jacopo Ciaffi; jacopo.ciaffi@unibo.it, jacopo.ciaffi@ior.it

† Equal contribution

ORCID IDs:

Jacopo Ciaffi: 0000-0002-9446-7351

Lorenzo Bianchi: 0009-0004-2584-707X

Marco Gambarotti: 0000-0002-8080-4484

Alberto Righi: 0000-0002-1074-0155

Dilia Giuggioli: 0000-0002-0041-3695

Roberto Caporali: 0000-0001-9300-6169

Cesare Faldini: 0000-0001-8152-4778

Stefano Zaffagnini: 0000-0002-2941-1407

Tom W J Huizinga: 0000-0001-7033-7520

Francesco Ursini: 0000-0001-8194-8642

ABSTRACT

Background: Synovial inflammation is increasingly recognized as a relevant component of osteoarthritis (OA), yet its histopathological and immunological features in advanced disease remain incompletely characterized. Whether distinct synovial pathotypes are associated with specific clinical, laboratory, radiographic characteristics, or postoperative outcomes is still unclear.

Methods: In this cross-sectional study, synovial tissue samples from OA patients undergoing hip or knee arthroplasty, or other joint surgery, were analyzed through standardized histology (Krenn score) and semi-quantitative immunohistochemistry (CD3, CD20, CD68, CD138). Pathotypes were categorized as lympho-myeloid, diffuse-myeloid, or pauci-immune. Preoperative demographics, Kellgren–Lawrence radiographic grade, systemic inflammatory markers, and postoperative outcomes were retrieved from clinical records. Comparisons were performed using Kruskal–Wallis and Fisher's exact tests. A multivariable logistic regression identified predictors of the lympho-myeloid pathotype.

Results: 244 samples were analyzed. High-grade synovitis was present in 64.3% of specimens. Pathotype distribution was: 55.3% lympho-myeloid, 11.9% diffuse-myeloid, and 32.8% pauci-immune. Lympho-myeloid tissues displayed the highest inflammatory burden, including elevated Krenn scores and higher systemic inflammatory indices. Pathotype distribution varied across joints, whereas the proportion of high-grade synovitis did not. In multivariable modeling, higher BMI increased the odds of lympho-myeloid pathotype (OR 1.11, 95%CI 1.01–1.22). No associations emerged for inflammatory markers, Kellgren–Lawrence grade or preoperative pain. Postoperative complications were not different across pathotypes.

Conclusions: Advanced OA displays marked synovial heterogeneity, with immune infiltration patterns that parallel systemic inflammatory signatures. Our findings support the concept that synovial pathotypes capture relevant biological variation within OA and may contribute to a more refined framework for disease stratification in future studies.

Keywords: osteoarthritis; pathotypes; inflammation; Krenn; synovitis.

BACKGROUND

Traditionally regarded as a degenerative "wear-and-tear" disorder, osteoarthritis (OA) is now recognized as a complex, multifactorial condition affecting the entire joint, including articular cartilage, subchondral bone, synovium, capsule, and periarticular tissues (1). Mechanical stress, aging, metabolic dysregulation, genetic predisposition, and low-grade inflammation interact in a self-perpetuating cycle leading to joint failure (2). The identification of distinct clinical phenotypes supports the concept that OA is not a single disease entity but rather a syndrome with heterogeneous pathogenic pathways (3).

Among these mechanisms, synovial inflammation has emerged as a central component of OA pathophysiology (4). Early descriptions portrayed OA-related synovitis as mild and secondary to cartilage wear; however, evidence accumulated over the last two decades demonstrates that inflammatory changes in the synovium are frequent, active, and clinically relevant (4). The cross-talk between subchondral bone and articular cartilage—particularly across the osteochondral junction—drives a cascade of angiogenesis, sensory nerve ingrowth, and release of pro-inflammatory mediators that amplify pain and structural deterioration (4–6). Within this microenvironment, cartilage-derived matrix fragments act as damage-associated molecular patterns (DAMPs), activating pattern-recognition receptors on chondrocytes and synoviocytes and sustaining the production of cytokines, chemokines, and proteases (7). These mediators, in turn, promote neovascularization and neo-innervation, contributing both to joint destruction and to nociceptive sensitization (8).

Imaging and histologic studies have consistently shown that synovitis is present in a substantial proportion of OA patients. Large-scale MRI studies have detected synovial thickening or enhancement in approximately 60% of subjects examined without contrast and up to 74% when contrast agents are used, with higher degrees of synovitis predicting faster cartilage loss (9–12). Histologic analyses confirm these findings, demonstrating synovial hyperplasia, stromal infiltration by mononuclear cells, and increased vascularity compared with healthy controls (13). Importantly, the severity of synovitis has been associated with both pain intensity and radiographic progression, suggesting that inflammation is not merely an epiphenomenon but an active driver of the disease (14–16).

A major advance in the histopathological characterization of synovitis came from the work of Krenn and colleagues, who proposed a semi-quantitative scoring system integrating lining-layer hyperplasia, stromal cellularity, and inflammatory infiltrate, allowing for standardized assessment of synovial inflammation (17,18). Building on the “Krenn score”, subsequent immunohistochemical research identified reproducible synovial pathotypes—lympho-myeloid, diffuse myeloid, and pauci-immune—based on the relative abundance of B cells, T cells, plasma cells, and macrophages in patients with rheumatoid arthritis (RA) (19–21).

These insights opened the possibility that similar inflammatory architectures might exist outside RA, and indeed a key breakthrough came from Boutet et al., who provided the first large-scale, systematic comparison between end-stage OA and RA synovium, challenging the assumption that complex immune infiltration is exclusive to autoimmune synovitis (22). Using both semi-quantitative and digital image analysis, they demonstrated that OA synovial tissue can be categorized into the same three pathotypes identified in RA, with the lympho-myeloid subtype present in more than half of OA cases undergoing joint replacement (22). Notably, OA and RA synovia exhibited overlapping distributions of Krenn grades, suggesting a continuum between degenerative and immune-mediated joint disease (22). This paradigm-switching study redefined the histopathological landscape of OA, revealing that adaptive immune cell aggregates and macrophage-rich infiltrates—once thought exclusive to RA—are frequent in OA and associate with peripheral blood cell indices consistent with low-grade systemic inflammation, such as lower hemoglobin and lymphocytes, and higher monocyte-to-lymphocyte ratio (MLR) and neutrophil-to-lymphocyte ratio (NLR).

However, the findings by Boutet and colleagues, while transformative, also raised several questions. Their cohort was large but geographically homogeneous (United Kingdom), and the clinical correlates of synovial pathotypes—such as radiographic severity, laboratory inflammation markers, or demographic determinants—were not fully explored. Moreover, all OA samples were derived from end-stage knee and hip disease, leaving uncertain whether the same inflammatory architecture applies across other joint

locations or different disease contexts. Independent validation in distinct populations, ideally using analogous standardized scoring and immunohistochemical approaches, is therefore essential to confirm the reproducibility of these observations.

In this context, our study aimed to characterize the histopathologic profile of synovial tissue obtained from patients with advanced OA undergoing orthopedic surgery at multiple joint sites—including the hip, knee, ankle, shoulder, elbow and wrist. Using standardized hematoxylin–eosin (H&E) and immunohistochemical staining, we quantified synovitis according to the Krenn score, defined synovial pathotype distribution, and investigated their associations with preoperative clinical, laboratory, and radiographic parameters, as well as with postoperative outcomes.

METHODS

Study design and setting

This study is a retrospective observational analysis of synovial tissue samples obtained from patients undergoing orthopedic surgery for OA at the IRCCS Istituto Ortopedico Rizzoli (Bologna, Italy), one of the largest European referral centers for musculoskeletal surgery. We identified all consecutive cases from January 2019 to December 2023 for which synovial tissue had been submitted to the Department of Pathology and stored in the institutional biobank.

A key methodological consideration is that synovial tissue is not routinely collected during arthroplasty or other OA-related procedures. In our institutional practice, sampling is performed when macroscopic inspection reveals synovitis that appears more prominent than typically expected in advanced OA. As a result, the synovial specimens included in the institutional biobank primarily derive from cases in which inflammatory features were clinically apparent, thereby providing a biologically informative subset of advanced OA enriched for synovial pathology rather than a random surgical sample.

We restricted inclusion to adult patients who underwent primary orthopedic surgery for clinically and radiographically confirmed OA involving synovial joints. While the study by Boutet et al. included RA comparators, the present cohort consists exclusively of OA cases and spans multiple anatomical sites — predominantly the hip and knee, but also the shoulder, ankle, elbow, and wrist (22). Synovial findings were further interpreted alongside perioperative clinical, laboratory, and radiographic data routinely collected in the surgical setting, including inflammatory biomarkers.

We applied stringent exclusion criteria to avoid confounding by alternative inflammatory or secondary degenerative processes. We excluded patients with any known chronic inflammatory arthropathy diagnosed, including RA, psoriatic arthritis, gout, axial spondyloarthritis, or other autoimmune rheumatic diseases. We also excluded secondary OA (post-traumatic, post-infectious, dysplastic, or post-fracture) and revision surgeries, including any case with prior implants, osteosynthesis, or earlier procedures involving the index joint.

Tissue processing and histological assessment

Synovial tissue samples were obtained intraoperatively at the time of orthopedic surgery and submitted to the Department of Pathology for routine diagnostic processing. Upon receipt, all specimens were fixed in 10% neutral-buffered formalin for a minimum of 24 hours, then dehydrated, cleared, and embedded in

paraffin following standard protocols. From each paraffin block, serial sections of 3–4 µm thickness were cut using a rotary microtome.

At least one section per case (typically 2 to 4 sections) was stained with H&E for general morphological evaluation. Tissue adequacy was defined as preserved morphology and a visible lining layer, according to standard pathology criteria (23). Sections lacking an identifiable synovial lining, with extensive cautery artifact, or consisting predominantly of dense fibrous tissue or adipose tissue were considered non-diagnostic and excluded from histological scoring. All evaluable H&E-stained slides were then digitized and independently reviewed by two trained readers (M.G. and A.R., senior musculoskeletal pathologists), both blinded to all clinical, laboratory, radiographic, and surgical data.

Histopathological evaluation of synovial tissue was performed on H&E–stained sections according to the Krenn synovitis score, a validated semi-quantitative system widely used to characterize inflammatory changes in both OA and inflammatory arthritides (18). Lining-layer hyperplasia, stromal cellularity, and inflammatory infiltrates were graded semi-quantitatively from 0 to 3 according to the Krenn synovitis score (18). Domain-specific scores were summed to obtain the total Krenn score (0–9) and classify synovitis as none (0–1), low grade (2–4), or high grade (≥5). Representative examples of the three inflammatory grades are shown in Figure 1A. All evaluable slides provided sufficient representation of both lining and sublining compartments to ensure reliable scoring across all three domains.

Immunohistochemistry and synovial pathotype classification

Immunohistochemical analyses were performed to characterize the cellular composition of the synovial inflammatory infiltrate.

First, 4-µm-thick tissue sections were cut, heated at 58 °C for 2 h, deparaffinized, and immunostained on a Ventana BenchMark following the manufacturer's guidelines (Ventana Medical Systems, Tucson, AZ, USA). Antibody detection was performed using UltraView Universal diaminobenzidine (DAB) detection kit (Ventana Medical Systems). Pretreatment for antigen retrieval was performed at 95°C with Tris–ethylenediamine tetraacetic acid (Tris-EDTA), pH8 for 20 min. When necessary, endogenous tissue peroxidase was blocked by treating the sections with 0.3% H_2O_2.

Four primary antibodies were used to identify the dominant immune cell lineages typically involved in synovial pathology: CD20 for B lymphocytes (L26; prediluted mouse monoclonal primary antibody; Ventana Medical Systems, Tucson, AZ, USA), CD3 for T lymphocytes (2GV6; prediluted rabbit monoclonal primary antibody; Ventana Medical Systems, Tucson, AZ, USA), CD138 for plasma cells (BA38, prediluted mouse monoclonal primary antibody; Cell Marque Tissue Diagnostics, Rocklin, CA, USA), and CD68 for macrophages (KP1; prediluted mouse monoclonal primary antibody; Ventana Medical Systems, Tucson, AZ, USA). Appropriate positive and negative controls were included in each run.

For each marker, staining was semi-quantitatively graded using a 0–4 scale, reflecting both the density and the architectural pattern of positive cells: 0 = absent or minimal staining; 1 = mild focal positivity; 2 = multifocal moderate infiltrates; 3 = dense aggregates or confluent areas of positivity; 4 = extensive sheet-like infiltration or prominent lymphoid/plasmacytic clusters.

Based on integration of the four markers, synovial tissues were classified into three predefined synovial pathotypes, consistent with established frameworks in synovial immunopathology (20):

1. Lympho-myeloid pathotype: prominent B-cell (CD20) and plasma-cell (CD138) infiltrates, accompanied by dense CD3+ T-cell aggregates and marked CD68+ macrophage presence.

2. Diffuse-myeloid pathotype: widespread macrophage predominance (CD68) with relatively sparse B- and plasma-cell infiltrates and variable T-cell density.
3. Pauci-immune/fibroid pathotype: minimal immune-cell staining across all markers, with synovial architecture dominated by fibroblast-like stromal elements and fibrotic remodeling.

Representative immunohistochemical patterns illustrating the three pathotypes are displayed in Figure 1B.

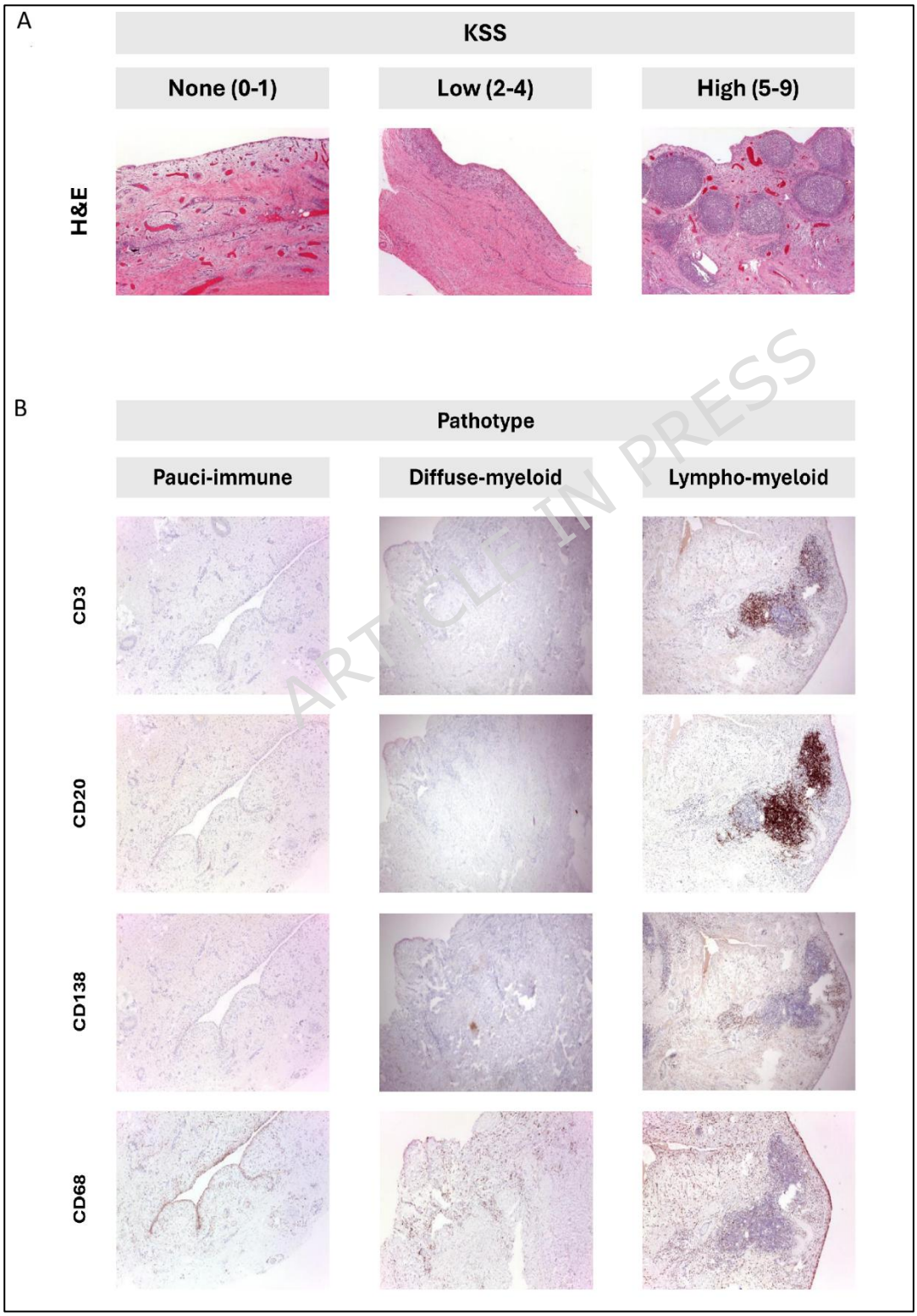

Figure 1. Histological grading of synovitis and immunohistochemical definition of synovial pathotypes in osteoarthritis.

(A). Sections of osteoarthritic synovium were stained with hematoxylin and eosin and graded according to the Krenn synovitis score (KSS) as *none* (0–1), *low-grade* (2–4), or *high-grade* (≥5) synovitis. Representative images are shown for each category.

(B). Serial sections of osteoarthritic synovium were stained with antibodies against CD3 (T cells), CD20 (B cells), CD138 (plasma cells), and CD68 (monocytes/macrophages). Representative immunohistochemical patterns are shown for each synovial pathotype (*pauci-immune*, *diffuse-myeloid*, and *lympho-myeloid*).

All images were acquired at an original magnification of 100×.

Clinical, laboratory, and radiographic variables

Clinical and demographic information was obtained from the institutional electronic medical records. Baseline was defined as the last preoperative clinical assessment occurring within three months before surgery. At this time point, the following variables were systematically recorded: age, sex, height, weight, and body mass index (BMI). Surgical data included the date of surgery, the type of procedure, laterality, and length of hospital stay.

Comorbidity burden was assessed using the Charlson Comorbidity Index (CCI), calculated from individual comorbidities (24). Laboratory data included complete blood count parameters and C-reactive protein (CRP), recorded preoperatively. From the differential blood count, we additionally calculated composite inflammatory indices widely used as markers of systemic inflammation, including the NLR, the platelet-to-lymphocyte ratio (PLR), and the systemic immune-inflammation index (SII) (25,26). Preoperative pain intensity was assessed using a numerical rating scale (NRS, 0–10), and the duration of joint pain was recorded in months. Radiographic severity of OA was evaluated using the Kellgren–Lawrence grading system, assigned on the basis of available preoperative radiographs (27). Kellgren–Lawrence grade was recorded on a 0–4 ordinal scale, reflecting the presence and progression of osteophytes, joint-space narrowing, subchondral sclerosis, and bone deformity. Radiographs were reviewed by an orthopedic surgeon and a rheumatologist.

Postoperative events were documented using predefined categories and were classified into short-term and long-term complications. Short-term complications were defined as those occurring during the index hospitalization or within 30 days after surgery. Long-term complications were defined as events occurring from postoperative month 2 up to the routine 12 ± 3-month follow-up visit.

Short-term events included the following predefined categories: postoperative bleeding requiring surgical treatment; failure of wound healing requiring reoperation; thromboembolic disease; postoperative neural deficit (sensory or motor); superficial periprosthetic joint infection; deep prosthetic joint infection; other medical complications including pneumonia, heart failure, urinary tract infection, arrhythmia, respiratory infection, or other relevant diagnoses.

Long-term complications were assessed through dedicated follow-up items and included: any reoperation; readmission; deep surgical infection.

Statistical analysis

Continuous variables were summarized as median and interquartile range (IQR), whereas categorical variables were reported as counts and percentages. Comparisons across synovial pathotypes (lympho-myeloid, diffuse-myeloid, pauci-immune) and across synovitis severity groups (low-grade vs. high-grade Krenn score) were conducted using the Kruskal–Wallis test for continuous variables and the Fisher's exact test for categorical variables. Whenever the Kruskal–Wallis test indicated significant overall differences, post-hoc pairwise comparisons were performed using Dunn's test with Bonferroni correction. For hemoglobin levels, additional multivariable linear regression analyses were performed to assess differences across synovial pathotypes after adjustment for sex.

Joint-specific analyses (knee, hip, other joints) were conducted to examine anatomical differences in synovial pathotype distribution and synovitis severity, again using Fisher's exact tests. Postoperative outcomes were summarized descriptively and compared across pathotypes using the same non-parametric testing strategy.

To explore independent predictors of the lympho-myeloid synovial pattern, a multivariable logistic regression model was fitted, including age, sex, BMI, preoperative NLR, PLR, CRP, hemoglobin, pain score, pain duration, CCI, Kellgren–Lawrence grade, and joint site (hip/knee/other). Results were expressed as odds ratios (ORs) with 95% confidence intervals (CIs). Multicollinearity was assessed using generalized variance inflation factors (GVIF), expressed as GVIF^(1/(2×Df)), with values <2 considered indicative of the absence of relevant multicollinearity. In addition, medication use during the year preceding surgery (including NSAIDs, systemic and intra-articular glucocorticoids, statins, metformin, and other antidiabetic agents) was summarized descriptively and explored across synovial pathotypes and CCI categories using contingency tables and Fisher's exact test.

All statistical tests were two-tailed, with a significance threshold of $p < 0.05$. All statistical analyses and figures 2–7 were generated using R (version 4.5.1), primarily with the packages broom (1.0.8), car (3.1.3), cowplot (1.1.3), dplyr (1.1.4), FSA (0.10.0), flextable (0.9.11), forcats (1.0.0), ggplot2 (3.5.2), gtsummary (2.4.0), haven (2.5.5), patchwork (1.3.0), purrr (1.0.4), rlang (1.1.6), tidyr (1.3.1), and tibble (3.3.0).

Ethical considerations

The research was conducted in accordance with the ethical principles of the 1964 Declaration of Helsinki and its later amendments (28). The study protocol was reviewed and approved by the Area Vasta Emilia Centro Ethics Committee (Comitato Etico AVEC) (approval code: CE-AVEC 732/2024/Sper/IOR).

All synovial specimens included in the analysis had been previously collected as part of routine diagnostic practice. Informed consent was sought from all eligible patients; written consent was obtained from those who could be reached. For patients who could not be contacted despite repeated attempts, the requirement for informed consent was waived by the Ethics Committee, in accordance with applicable regulations for retrospective research involving previously collected biological material, when obtaining consent is not feasible and the research entails minimal risk to participants, as outlined in the Declaration of Helsinki (paragraph 32).

Clinical data were extracted from institutional electronic medical records and managed using the REDCap electronic data capture system, in full compliance with the European Union General Data Protection Regulation (EU GDPR 2016/679) and local data-protection policies. All data were de-identified prior to analysis, and access was restricted to authorized members of the research team.

RESULTS

Patient characteristics

A total of 244 patients were included in the study. The main characteristics of the study population are presented in Table 1. The median age was 68.4 years (IQR 60.9–76.5), and 56.6% were women. The median BMI was 26.5 kg/m² (IQR 24.2–30.2). Most procedures involved large weight-bearing joints: 68.4% of patients underwent knee replacement and 25% hip replacement, whereas shoulder replacement (2.1%), ankle arthrodesis or replacement (2.5%), elbow arthrolysis (1.6%), and wrist arthrodesis (0.4%) were less common.

Radiographic severity was substantial, with a median Kellgren–Lawrence grade of 3 (IQR 3–4). Preoperative pain severity was high, with a median NRS of 6 (IQR 5–8). Information on pain duration before surgery was available for 163 patients, showing a median duration of 24 months (IQR 12–60). Systemic inflammatory activity was generally low, reflected by a median CRP of 0.28 mg/dL (IQR 0.13–0.51). Hematological parameters showed median neutrophil and lymphocyte counts of 4.1×10^9/L (IQR 3.3–5.0) and 1.8×10^9/L (IQR 1.4–2.2), respectively, a median platelet count of 236×10^9/L (IQR 195–279), and a median hemoglobin level of 13.8 g/dL (IQR 12.9–14.7).

Comorbidity burden was moderate: among patients with available data (n = 241), 58.1% had a CCI of 0, 30.3% had a CCI of 1–2, and 11.6% had a CCI ≥3. The most frequent comorbidities included chronic pulmonary disease (17.2%), peripheral vascular disease (8.2%), congestive heart failure (7.8%), prior myocardial infarction (6.6%) and diabetes (5.7%). Patients with any comorbidity (CCI ≥1) were significantly older than those without comorbidities (median 73.9 years [IQR 65.1–78.0] vs 66.1 years [58.1–72.9], p<0.001).

Table 1. Baseline demographic, clinical, laboratory, and histopathological characteristics of the study population overall and according to synovial pathotype.

Variable	Overall (n=244)	Lympho-myeloid (n=135)	Diffuse-myeloid (n=29)	Pauci-immune (n=80)	p-value [1]
Age, years, median (IQR)	68.4 (60.9–76.5)	70.6 (62.5–77.4)	67.0 (63.2–73.8)	67.3 (57.6–74.9)	0.038
Female sex, n (%)	138 (56.6%)	87 (64.4%)	11 (37.9%)	40 (50.0%)	0.012
BMI, kg/m², median (IQR	26.5 (24.2–30.2)	27.1 (24.7–31.2)	25.6 (24.1–28.1)	25.9 (23.9–29.4)	0.120

Variable	Overall (n=244)	Lympho-myeloid (n=135)	Diffuse-myeloid (n=29)	Pauci-immune (n=80)	p-value [1]
Kellgren–Lawrence grade					0.037
1	3 (1.2%)	0 (0.0%)	2 (6.9%)	1 (1.3%)	
2	42 (17.2%)	18 (13.3%)	4 (13.8%)	20 (25.0%)	
3	88 (36.1%)	54 (40.0%)	8 (27.6%)	26 (32.5%)	
4	111 (45.5%)	63 (46.7%)	15 (51.7%)	33 (41.3%)	
Preoperative pain NRS, median (IQR)	6.0 (5.0–8.0)	6.0 (5.0–8.0)	6.0 (5.0–7.0)	6.0 (5.0–7.0)	0.059
Pain duration, months, median (IQR) *	24.0 (12.0–60.0)	24.0 (12.0–66.0)	18.0 (11.0–48.0)	36.0 (12.0–48.0)	0.424
CRP, mg/dL	0.28 (0.13–0.51)	0.34 (0.13–0.61)	0.26 (0.20–0.39)	0.23 (0.12–0.38)	0.033
Neutrophils, $\times 10^9$/L	4.1 (3.3–5.0)	4.3 (3.4–5.7)	4.3 (3.7–5.0)	3.7 (3.1–4.4)	0.003
Lymphocytes, $\times 10^9$/L	1.8 (1.4–2.2)	1.8 (1.5–2.1)	1.8 (1.3–2.2)	1.8 (1.5–2.4)	0.779
Platelets, $\times 10^9$/L	236 (195–279)	254 (214–299)	225 (185–271)	210 (179–248)	<0.001
Hemoglobin, g/dL	13.8 (12.9–14.7)	13.5 (12.7–14.4)	14.2 (13.2–15.0)	14.3 (13.6–14.8)	<0.001
NLR	2.28 (1.59–3.08)	2.42 (1.72–3.31)	2.28 (2.04–2.87)	2.03 (1.51–2.57)	0.003
PLR	133 (102–170)	139 (113–179.0)	141 (93–165)	119 (92–151)	0.003
SII	526 (363–753)	576 (410–900)	535 (363–711)	454 (286–602)	<0.001
Charlson Comorbidity Index, n (%) **					0.614
0	140 (58.1%)	74 (55.2%)	17 (58.6%)	49 (62.8%)	
1–2	73 (30.3%)	46 (34.3%)	8 (27.6%)	19 (24.4%)	
≥3	28 (11.6%)	14 (10.4%)	4 (13.8%)	10 (12.8%)	
Main comorbidities,					

Variable	Overall (n=244)	Lympho-myeloid (n=135)	Diffuse-myeloid (n=29)	Pauci-immune (n=80)	p-value [1]
n (%)					
Prior myocardial infarction	16 (6.6%)	9 (6.7%)	1 (3.4%)	6 (7.5%)	0.873
Congestive heart failure	19 (7.8%)	11 (8.1%)	2 (6.9%)	6 (7.5%)	1.000
Peripheral vascular disease	20 (8.2%)	14 (10.4%)	3 (10.3%)	3 (3.8%)	0.193
Chronic pulmonary disease	42 (17.2%)	25 (18.5%)	3 (10.3%)	14 (17.5%)	0.650
Diabetes	14 (5.7%)	7 (5.2%)	1 (3.4%)	6 (7.5%)	0.723
Histopathological evaluation					
Krenn score, median (IQR)	5.0 (4.0–6.0)	6.0 (5.0–6.0)	5.0 (4.0–6.0)	4.0 (3.0–5.0)	<0.001
Synovitis grade, n (%)					<0.001
Low-grade	87 (35.7%)	31 (23.0%)	8 (27.6%)	48 (60.0%)	
High-grade	157 (64.3%)	104 (77.0%)	21 (72.4%)	32 (40.0%)	

[1] P-values refer to overall comparisons across the three synovial pathotype groups (lympho-myeloid, diffuse-myeloid, and pauci-immune), using the Kruskal–Wallis test for continuous variables and Fisher's exact test for categorical variables.

Data are presented as median (interquartile range, IQR) for continuous variables and number (percentage) for categorical variables. Percentages are calculated on the total study population unless otherwise specified. Missing values are reported where applicable.

Comparisons across synovial pathotype groups were performed using the Kruskal–Wallis test for continuous variables and Fisher's exact test for categorical variables.

CCI: Charlson Comorbidity Index; CRP: C-reactive protein; NLR: neutrophil-to-lymphocyte ratio; PLR: platelet-to-lymphocyte ratio; SII: systemic immune-inflammation index.

* Available in 163 patients (68% of the cohort).

** Percentages are calculated based on available data (n = 241).

Histological and immunohistochemical characteristics

Histological assessment showed a substantial inflammatory burden within the synovial tissues. The overall median Krenn score was 5 (IQR 4–6), with 64.3% of samples classified as high-grade synovitis and 35.7% as low-grade synovitis (Figure 2A). No specimen met criteria for absent synovitis. Most tissues displayed at least moderate lining-layer hyperplasia, increased stromal cellularity, and mononuclear infiltrates of grade ≥1, consistent with widespread active synovitis.

Based on the combined distribution of immune cell subsets, the lympho-myeloid pattern was the most prevalent (55.3%), followed by the pauci-immune pattern (32.8%) and the diffuse-myeloid pattern (11.9%). Semi-quantitative distributions of the individual immunohistochemical markers used to define synovial pathotypes (CD3, CD20, CD68, and CD138) are reported in Supplementary Table 1, while the distribution of pathotypes in the cohort is shown in Figure 2B. Notably, all three categories included both low- and high-grade Krenn scores, but the prevalence of high-grade synovitis differed substantially across pathotypes from 77.0% of lympho-myeloid to 72.4% of diffuse-myeloid, and 40.0% of pauci-immune samples (Fisher $p<0.0001$; Figure 2C).

Consistently, a clear gradient in histological inflammation emerged across pathotypes. Median Krenn scores increased from 4 (IQR 3–5) in pauci-immune tissues to 5 (IQR 4–6) in diffuse-myeloid and 6 (IQR 5–6) in lympho-myeloid tissues (Kruskal–Wallis $p<0.001$). Post-hoc Dunn tests confirmed higher Krenn scores in lympho-myeloid and diffuse-myeloid tissues compared with pauci-immune ($p<0.001$ and $p=0.001$, respectively), with no significant difference between the two myeloid-rich groups. These comparisons are illustrated in Figure 2D.

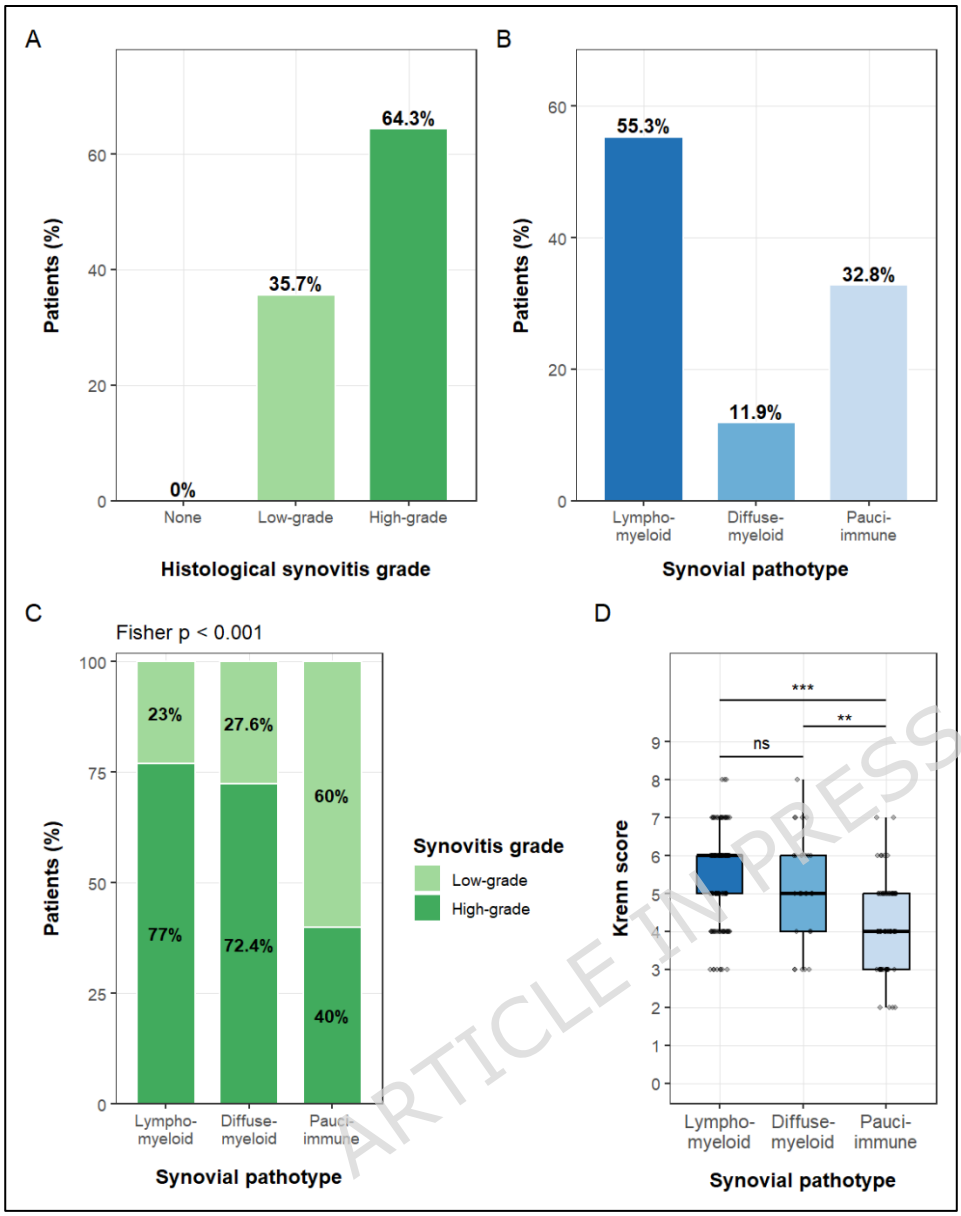

Figure 2. Histological severity, synovial pathotypes, and inflammatory gradients in osteoarthritis synovium.

(A). Distribution of histological synovitis grades based on the Krenn score.

(B). Prevalence of the three synovial pathotypes.

(C). Cross-classification of synovitis grade and synovial pathotype.

(D). Comparison of median Krenn scores across pathotypes.

Pairwise comparisons for panel D (Dunn's test with Bonferroni correction) showed: lympho-myeloid vs pauci-immune ($p < 0.001$), diffuse-myeloid vs pauci-immune ($p = 0.001$), and lympho-myeloid vs diffuse-myeloid ($p = 1.000$).

Significance annotation: ** $p < 0.01$; *** $p < 0.001$

Association between synovial pathotypes and clinical, laboratory or radiographic parameters

We next evaluated whether clinical, laboratory, and radiographic parameters differed across synovial pathotypes (Figure 3A–H).

Age (Figure 3A) showed modest variation across groups (Kruskal–Wallis p=0.038). Patients with a lympho-myeloid pathotype were slightly older (median 70.6 years, IQR 62.5–77.4) than those with a pauci-immune pattern (median 67.3 years, IQR 57.6–74.9), with a significant overall difference (p=0.038). BMI (Figure 3B) did not differ significantly across pathotypes (p=0.120). Preoperative pain NRS (Figure 3C) was similar across all groups (p=0.059). Hemoglobin (Figure 3D) differed significantly across pathotypes (Kruskal–Wallis p<0.001). Median hemoglobin was lowest in the lympho-myeloid group (13.5 g/dL, IQR 12.7–14.4), intermediate in diffuse-myeloid tissues (14.2 g/dL, IQR 13.2–15.0), and highest in the pauci-immune group (14.3 g/dL, IQR 13.6–14.8). Post-hoc comparisons confirmed significantly lower hemoglobin in lympho-myeloid versus pauci-immune synovium (p<0.001). This difference remained significant after adjustment for sex in a multivariable linear regression model.

A clear gradient was observed for systemic inflammatory indices. NLR (Figure 3E) increased progressively from the pauci-immune (median 2.03, IQR 1.51–2.57), to the diffuse-myeloid (2.28, IQR 2.04–2.87), and to the lympho-myeloid pattern (2.42, IQR 1.72–3.31), with a significant overall difference (p=0.003). Lympho-myeloid samples displayed higher NLR than pauci-immune tissues (p=0.003). PLR (Figure 3F) also differed significantly across groups (p=0.003). Values were highest in lympho-myeloid tissues (median 139, IQR 113–179) and lowest in the pauci-immune group (median 119, IQR 92–151), with a significant overall difference (p=0.003). SII (Figure 3G) followed a similar trend, increasing from pauci-immune (454, IQR 286–602) to diffuse-myeloid (535, IQR 363–711), and to lympho-myeloid samples (576, IQR 410–900). The overall comparison was significant (p<0.001), and lympho-myeloid tissues had higher SII than pauci-immune specimens (p<0.001). CRP (Figure 3H) varied across groups (p=0.033), with higher values in lympho-myeloid (0.34 mg/dL, IQR 0.13–0.61) compared with pauci-immune synovium (0.23 mg/dL, IQR 0.12–0.38; post-hoc p = 0.030). No significant differences emerged between lympho-myeloid and diffuse-myeloid samples for any parameter.

Kellgren–Lawrence grades differed significantly across pathotypes (Fisher's exact test p=0.037). The proportion of grades 3–4 (Figure 4A) appeared progressively higher from pauci-immune (73.7%) to diffuse-myeloid (79.3%) and to lympho-myeloid synovium (86.7%).

To further explore systemic–local inflammatory links, we stratified the cohort into CRP tertiles and evaluated the distribution of synovial pathotypes and histological synovitis. Histological grades across CRP tertiles (Figure 4B) showed a non-significant trend (Fisher p=0.092), with high-grade synovitis increasing from 54.9% (lowest tertile) to 67.9% (middle tertile) and to 70.4% (highest tertile). Pathotypes across CRP tertiles (Figure 4C) showed a significant overall difference (Fisher p=0.002), with the pauci-immune pattern becoming progressively less frequent in the highest CRP tertile (from 39% to 35.8% to 23.5%).

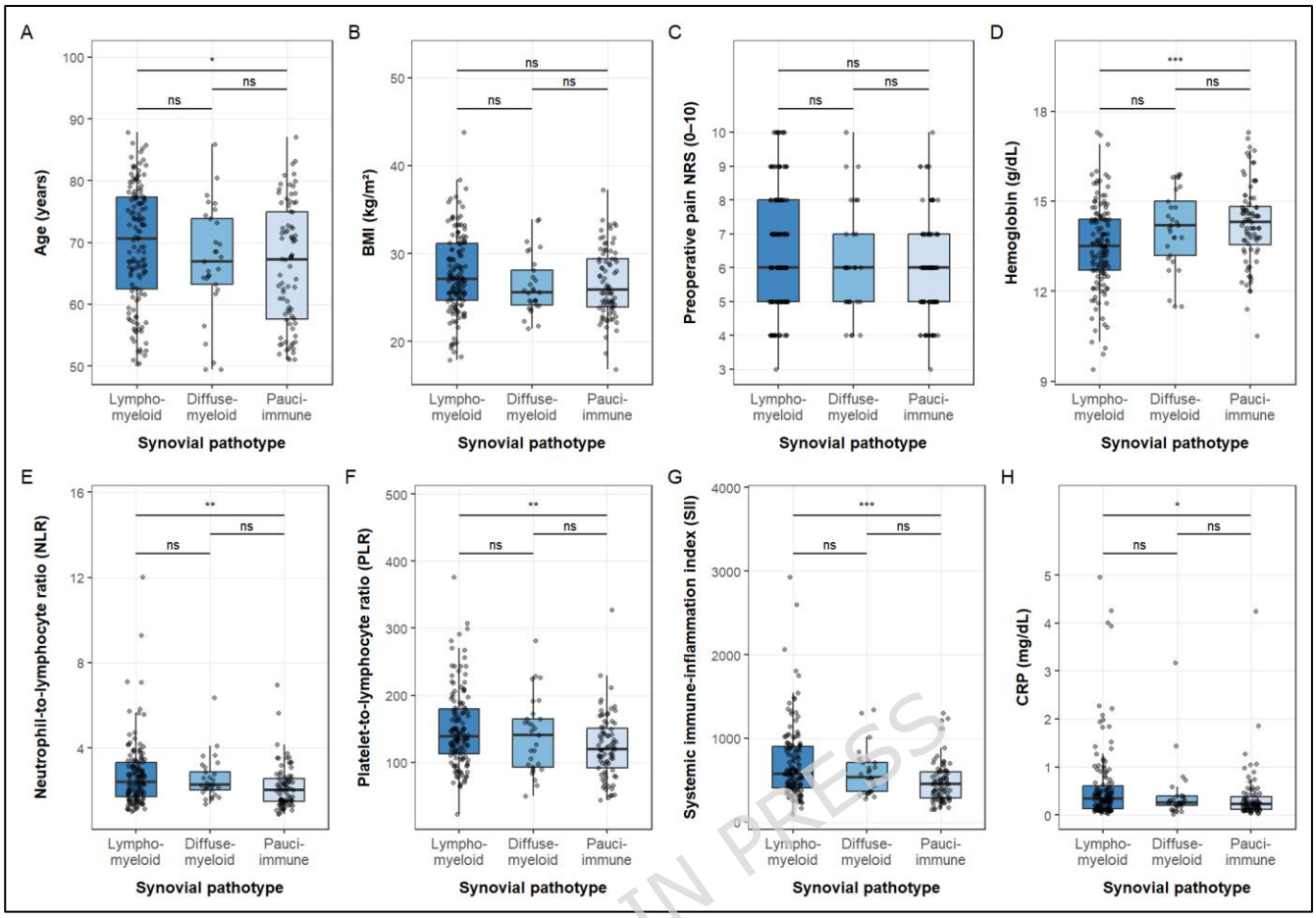

Figure 3. Clinical and laboratory characteristics across synovial pathotypes.

Boxplots showing the distribution of eight key clinical and laboratory variables across the three synovial pathotypes:

(A). Age

(B). BMI

(C). Preoperative pain numerical rating scale

(D). Hemoglobin

(E). Neutrophil-to-lymphocyte ratio (NLR)

(F). Platelet-to-lymphocyte ratio (PLR)

(G). systemic immune-inflammation index (SII)

(H). C-reactive protein

Pairwise comparisons (Dunn's test with Bonferroni correction) showed:

Age (A): lympho-myeloid vs pauci-immune (p = 0.049), diffuse-myeloid vs lympho-myeloid (p = 0.433), diffuse-myeloid vs pauci-immune (p = 1.000).

BMI (B): lympho-myeloid vs pauci-immune (p = 0.254), diffuse-myeloid vs lympho-myeloid (p = 0.376), diffuse-myeloid vs pauci-immune (p = 1.000).

Pain NRS (C): lympho-myeloid vs pauci-immune (p = 0.056), diffuse-myeloid vs lympho-myeloid (p = 1.000), diffuse-myeloid vs pauci-immune (p = 1.000).

Hemoglobin (D): lympho-myeloid vs pauci-immune (p < 0.001), diffuse-myeloid vs lympho-myeloid (p = 0.086), diffuse-myeloid vs pauci-immune (p = 1.000).

NLR (E): lympho-myeloid vs pauci-immune (p = 0.003), diffuse-myeloid vs lympho-myeloid (p = 1.000), diffuse-myeloid vs pauci-immune (p = 0.076).

PLR (F): lympho-myeloid vs pauci-immune (p = 0.002), diffuse-myeloid vs lympho-myeloid (p = 1.000), diffuse-myeloid vs pauci-immune (p = 0.519).

SII (G): lympho-myeloid vs pauci-immune (p < 0.001), diffuse-myeloid vs lympho-myeloid (p = 1.000), diffuse-myeloid vs pauci-immune (p = 0.121).

CRP (H): lympho-myeloid vs pauci-immune (p = 0.030), diffuse-myeloid vs lympho-myeloid (p = 0.810), diffuse-myeloid vs pauci-immune (p = 1.000).

Significance annotation: * p < 0.05; ** p < 0.01; *** p < 0.001

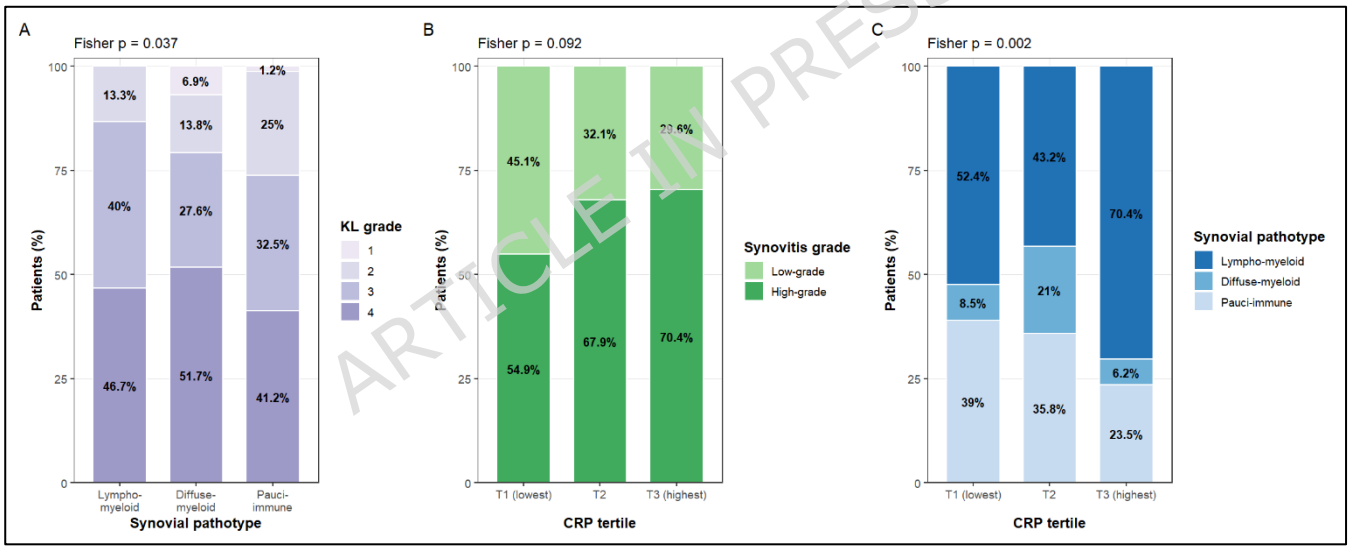

Figure 4. Kellgren–Lawrence grade and inflammatory profiles in relation to CRP tertiles.

(A). Distribution of Kellgren–Lawrence grades across the three synovial pathotypes.

(B). Distribution of Krenn synovitis grades across CRP tertiles.

(C). Distribution of synovial pathotypes across CRP tertiles.

Statistical analysis: Fisher's exact test (panel A: p = 0.037; panel B: p = 0.092; panel C: p = 0.002).

Multivariable analysis of predictors of the lympho-myeloid pathotype

To explore independent predictors of synovial inflammation patterns, we performed a multivariable logistic regression including preoperative demographic, clinical, laboratory and radiographic variables, using the lympho-myeloid pattern as the dependent outcome.

In the fully adjusted model (Figure 5), BMI remained the only variable positively associated with higher odds of exhibiting a lympho-myeloid synovial pathotype (OR 1.11, 95% CI 1.01–1.22, p=0.028). Conversely, a higher CCI was independently associated with lower odds of having a lympho-myeloid pattern (OR 0.70, 95% CI 0.50–0.97, p=0.036).

No significant associations emerged for age, sex, NLR, PLR, CRP, hemoglobin, preoperative pain intensity, pain duration, or joint site. Kellgren–Lawrence grade showed a trend toward higher odds of lympho-myeloid infiltration (OR 1.54, 95% CI 0.96–2.51) but did not reach statistical significance (p=0.074). The full results of the multivariable logistic regression model are presented in Supplementary Table 2, including ORs, 95% CIs, and p-values for all included covariates.

Exploratory analyses of medication use in the year preceding surgery showed no significant differences across synovial pathotypes. In contrast, statins, metformin, and other antidiabetic agents were progressively more frequent with increasing CCI category (statins: 0% in CCI 0, 37.0% in CCI 1–2, and 85.7% in CCI ≥3; metformin: 0%, 11.0%, and 21.4%; other antidiabetics: 0%, 8.2%, and 10.7%; all $p < 0.001$), supporting a close relationship between comorbidity burden and cardiometabolic treatment exposure.

Multicollinearity diagnostics showed no evidence of concerning collinearity among the variables included in the multivariable model); detailed results are reported in Supplementary Table 3.

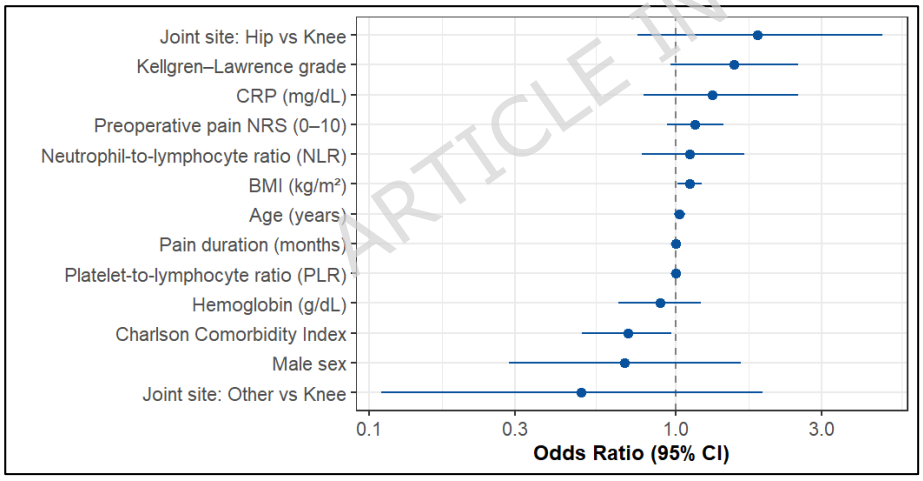

Figure 5. Forest plot of the multivariable logistic regression model evaluating independent predictors of the lympho-myeloid synovial pathotype. Odds ratios are presented with 95% confidence intervals.

Joint-specific synovial characteristics

High-grade synovitis was observed in 63.5% of knee samples (n=167), 65.6% of hip samples (n=61), and 68.8% of specimens from other joints (n=16). Fisher's exact test (p=0.924) did not show a significant association between joint site and histological grade (Figure 6A).

Among knee samples, the distribution of pathotypes was: 52.7% lympho-myeloid, 14.4% diffuse-myeloid, and 32.9% pauci-immune. Hip specimens displayed a similar predominance of lympho-myeloid tissue (68.9%), whereas diffuse-myeloid infiltration was less frequent (4.9%). In the other joints, the pauci-immune pattern was relatively more common (56.2%). A global comparison (Figure 6B) confirmed a statistically significant difference in pathotype distribution across anatomical sites (Fisher's exact test p=0.025). Exploratory pairwise comparisons showed a statistically significant difference between hip and other joints (Bonferroni-adjusted p = 0.048), whereas no significant differences were observed for the other comparisons (knee vs hip Bonferroni-adjusted p = 0.147, knee vs other joints Bonferroni-adjusted p = 0.547).

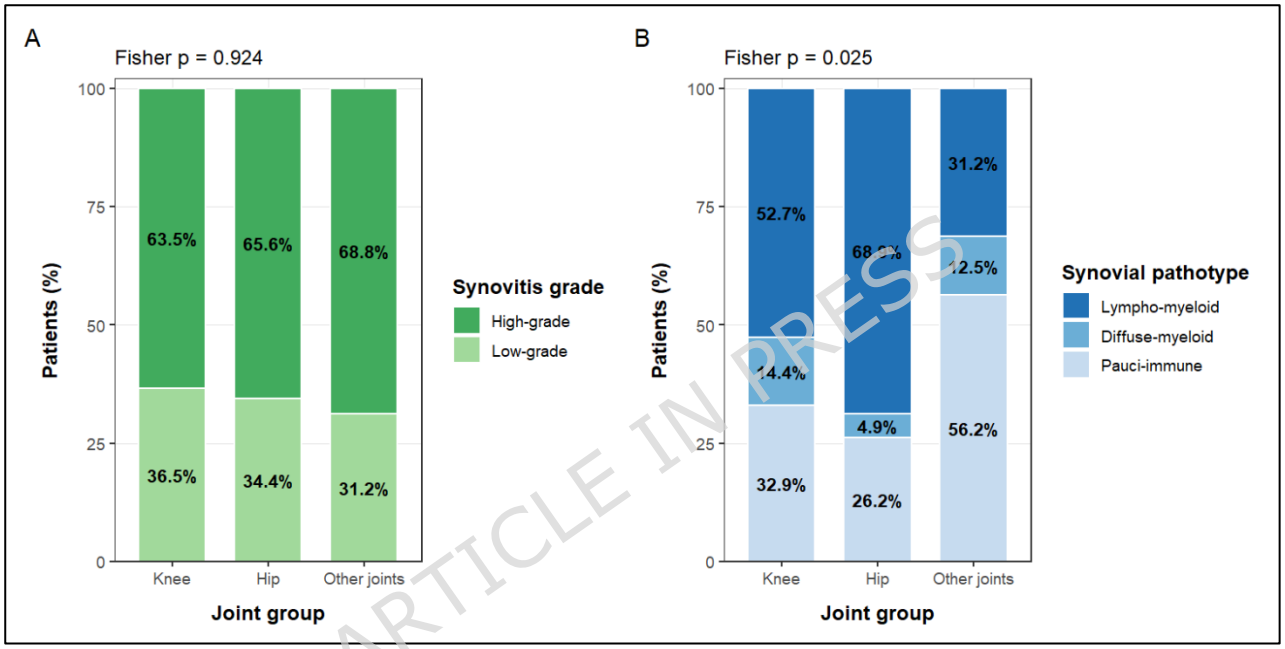

Figure 6. Synovial pathotypes and histological synovitis severity across joint sites. "Other joints" include shoulder, ankle, elbow, and wrist.

(A). Distribution of synovitis severity across joint sites.

(B). Distribution of synovial pathotypes across joint sites.

Statistical analysis: Fisher's exact test (panel A: p = 0.924; panel B: p = 0.025).

Postoperative course and follow-up

Short-term (30 days) complications—including wound-healing failure, superficial or deep postoperative infection, venous thromboembolism, fever, bleeding requiring transfusion, urinary tract infections, respiratory tract infections, and perioperative arrhythmias—collectively occurred in 31 patients (12.7%) (Figure 7A).

Information regarding late complications (from the second month to 1-year follow-up) was available in 175 patients (71.7%). Among these, 15 patients (8.6%) experienced at least one late complication. The most frequent events were revision surgery (3.7%), hospital readmission (3.7%), deep surgical infection (2.0%), and reoperation for any cause (0.8%) (Figure 7A). No significant differences were observed in the occurrence of either early (p=0.624) or late complications (p=0.081) across the three synovial pathotypes.

Hospital stay had a median duration of 7 days (IQR 6–8). Length of stay differed modestly across synovial pathotypes: 7 days (IQR 6–8) for lympho-myeloid tissue, 6 days (IQR 5–8) for diffuse-myeloid, and 7 days (IQR 6–7) for pauci-immune samples (Figure 7B). While the global Kruskal–Wallis test indicated statistical significance (p = 0.039), no pairwise comparison remained significant after Bonferroni correction.

Follow-up pain scores were available for 167 patients (68.4%). The overall median pain NRS was 2 (IQR 1–3), with comparable values across synovial pathotypes: 2 (IQR 1–3) in lympho-myeloid tissue, 2 (IQR 1–2.75) in diffuse-myeloid, and 2 (IQR 1–3) in pauci-immune samples (Figure 7C). No significant differences were observed (Kruskal–Wallis p = 0.536).

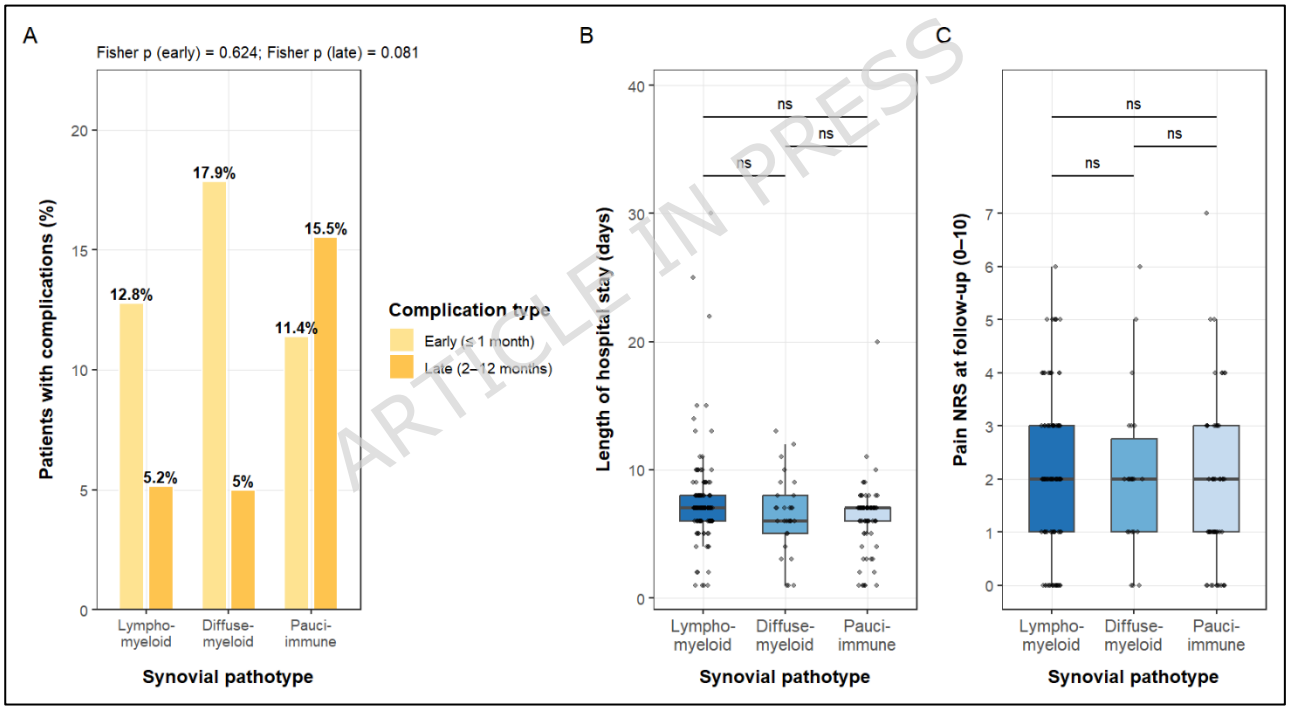

Figure 7. Postoperative complications, hospital stay, and follow-up pain across synovial pathotypes.

(A). Distribution of early and late postoperative complications according to synovial pathotype.

(B). Median length of hospital stay according to synovial pathotype.

(C). Median pain intensity at 12 ± 3-month follow-up (NRS 0–10).

Pairwise comparisons (Dunn's test with Bonferroni correction) showed:

Length of hospital stay (B): lympho-myeloid vs pauci-immune (p = 0.063), diffuse-myeloid vs lympho-myeloid (p = 0.316), diffuse-myeloid vs pauci-immune (p = 1.000).

Follow-up pain (C): lympho-myeloid vs pauci-immune (p = 0.793), diffuse-myeloid vs lympho-myeloid (p = 1.000), diffuse-myeloid vs pauci-immune (p = 1.000).

DISCUSSION

OA is increasingly recognized as a heterogeneous disease with substantial inflammatory involvement, challenging its historical view as a purely degenerative disorder (29). Over the past decade, several studies have demonstrated that synovial inflammation is not only common but also contributes to pain, disease progression, and postoperative outcomes in patients undergoing joint replacement (30–32). Histopathological analyses consistently show variable degrees of lining-layer hyperplasia, stromal activation, and immune cell infiltration within OA synovium, supporting the concept that OA encompasses distinct inflammatory pathotypes rather than a uniform pathological process (33–35).

In this context, our study provides a comprehensive characterization of synovial inflammation in a large cohort of patients undergoing surgery for advanced OA. Consistent with previous reports, we observed a high prevalence of histological synovitis, with 64.3% of samples classified as high-grade synovitis (22). This reinforces the notion that significant inflammatory activity persists in advanced OA, as previously observed (29). Importantly, while the prevalence of the lympho-myeloid subtype in our cohort closely mirrors that reported by Boutet et al., we observed a higher proportion of pauci-immune cases and a lower frequency of diffuse-myeloid pathotype (22). These differences may reflect distinct characteristics of the study populations: unlike Boutet et al., who focused exclusively on end-stage hip and knee OA, our cohort also included other joints (ankle, wrist, elbow, and shoulder), where the pauci-immune pattern was more prevalent. However, these findings should be interpreted with caution given the limited number of cases and the potential lack of statistical power to detect subtle joint-specific differences. Moreover, our cohort encompassed a broader spectrum of disease severity, including patients with non-advanced radiographic OA. Notably, among patients classified as pauci-immune, approximately one-quarter (26.2%) had a Kellgren–Lawrence grade of 1 or 2, a numerically higher proportion compared to the other two pathotypes. Taken together, these differences may account for the divergent distribution of diffuse-myeloid and pauci-immune pathotypes observed in our study relative to that of Boutet et al. (22).

In interpreting these findings, it is important to consider that the observed distribution of synovial pathotypes is influenced by both disease severity and sampling strategy. Our study population consisted of patients undergoing surgery for symptomatic OA with significant pain or functional impairment, encompassing a spectrum of radiographic severity, and representing a setting inherently enriched for clinically relevant inflammatory features. Moreover, inclusion in the histological analysis was contingent upon intraoperative macroscopic identification of prominent synovial inflammation, such that only cases with visibly inflamed synovial tissue were selected, resulting in a targeted enrichment of inflammatory phenotypes within the study cohort.

Across the literature, the burden of synovial inflammation varies substantially depending on disease stage and study design. Studies conducted in non-end-stage OA populations using minimally invasive biopsy approaches have reported markedly lower levels of histological synovitis, with only a small proportion of patients exhibiting high-grade inflammation in cohorts characterized by lower radiographic severity (36). Conversely, studies based on surgical specimens from advanced OA tend to report higher inflammatory burden (22,37). However, the extent to which these cohorts represent consecutive, unselected surgical populations, is not always explicitly detailed, which may contribute to variability in reported prevalence.

Importantly, beyond differences in patient selection, synovial inflammation has been shown to exhibit significant intra-articular heterogeneity. Variability in histological synovitis scores across different biopsy locations within the same joint has been reported, with some patients displaying both low-grade and high-grade synovitis in distinct regions of the same joint (38). This spatial heterogeneity further complicates the interpretation of synovial prevalence as a fixed property.

These observations suggest that the distribution of synovial pathotypes should be interpreted as a context-dependent feature, influenced by disease severity, clinical setting, and tissue sampling strategy, rather than as a uniform characteristic of OA. This concept is further supported by histopathological studies showing that synovial inflammation contributes to defining distinct OA subgroups across the disease spectrum (39). Our findings further demonstrate a stepwise increase in histological inflammation across pathotypes, with lympho-myeloid tissues showing the highest Krenn scores, intermediate values in diffuse-myeloid, and the lowest burden in pauci-immune synovium. This gradient corroborates the hierarchical inflammatory stratification described by previous work in both OA and RA synovium and further supports the potential biological relevance of synovial pathotypes beyond descriptive categorization (22,40–42).

We also found that lympho-myeloid tissues were associated with elevated systemic inflammatory indices, including higher NLR, PLR, and SII, as well as higher CRP and lower hemoglobin—an observation in line with the study by Boutet et al., who reported similar associations between lymphoid-rich OA synovium and systemic inflammation (22). However, while statistically significant, the observed differences are modest in magnitude and are unlikely to be clinically meaningful at the individual patient level. Rather, they may reflect consistent group-level differences in systemic inflammatory burden, reinforcing the concept that synovial pathotypes reflect not only local tissue biology but also broader inflammatory signatures (43,44).

Although BMI did not differ significantly across synovial pathotypes in non-parametric comparisons of median values, in multivariable analysis it emerged as an independent predictor of exhibiting a lympho-myeloid synovial pathotype. Conversely, the Kellgren–Lawrence grade, which showed significant differences across pathotypes in categorical analyses, did not retain independent significance after adjustment. This apparent discrepancy likely reflects the partial overlap between metabolic and structural dimensions of OA severity, supported by a weak but directionally consistent correlation between increasing BMI and higher Kellgren–Lawrence radiographic grade in our cohort. The association between adiposity and synovial inflammation aligns with the established role of metabolic–inflammatory pathways in OA, including adipokine dysregulation, chronic low-grade systemic inflammation, and altered macrophage polarization (45,46). These findings highlight potential systemic determinants of synovial immunopathology that warrant further mechanistic investigation.

Interestingly, the same multivariable model yielded a seemingly counterintuitive result, whereby higher CCI scores were associated with lower odds of exhibiting a lympho-myeloid synovial pathotype. A possible interpretation is that these older, multimorbid patients have senescent adaptive immune systems, which are less capable of orchestrating the highly organized tertiary lymphoid structures that characterize lymphoid-rich synovitis (47). In parallel, the same patients are disproportionately exposed to medications with systemic anti-inflammatory or immunomodulatory properties, such as statins, metformin, or low-dose aspirin and, in some cases, chronic low-dose glucocorticoids, all of which may blunt synovial inflammation (48). In line with this, we observed a progressive increase in the use of statins and antidiabetic agents across CCI categories in our cohort, supporting a link between comorbidity burden and cardiometabolic treatment exposure. However, given the observational nature of our data, no causal inference can be made regarding a potential influence of these medications on synovial pathotype. Moreover, long-standing diabetes, atherosclerosis and other CCI-defining comorbidities are established drivers of microangiopathy

and chronic tissue hypoxia, that in turn may promote a shift from a cellular, immune-infiltrated synovium towards a more fibrotic, hypocellular, “burnt-out” stroma as suggested in other tissues (49). Finally, selection bias cannot be excluded. Patients with high CCI scores typically undergo arthroplasty only after a rigorous risk–benefit assessment, such that those who reach surgery may represent a subset in whom structural damage and mechanical symptoms, rather than highly active inflammatory synovitis, are the predominant drivers of the surgical indication.

Crucially, we found no differences in hospital length of stay, early complications, late complications, or postoperative pain at follow-up across synovial pathotypes. At least in the context of advanced OA, marked synovial inflammation does not appear to translate into worse perioperative course or short-term clinical outcomes.

From a clinical perspective, these findings suggest that synovial pathotypes have limited immediate implications for patient management. In our cohort, the absence of differences in perioperative course and short-term clinical outcomes across pathotypes indicates that their relevance does not extend to current surgical decision-making. However, these observations support the concept that OA comprises biologically heterogeneous inflammatory patterns. Synovial pathotyping may represent a useful framework for future research aimed at better understanding disease heterogeneity and refining patient stratification. Any potential role in guiding therapeutic strategies remains to be established.

Recent high-dimensional studies further support the view that synovial inflammatory architecture extends beyond purely descriptive morphology. In RA, multimodal single-cell analyses have identified cell-type abundance phenotypes associated with histological features and treatment response, suggesting that classical histological pathotypes may represent morphologically accessible correlates of a deeper cellular organization (50). In this perspective, our findings do not compete with single-cell frameworks, but are conceptually aligned with them. In OA, emerging single-cell studies have begun to characterize cellular heterogeneity across joint tissues, highlighting shifts toward pro-inflammatory macrophage populations and alterations in regenerative cell compartments (51,52). However, compared to RA, these data remain less standardized and lack a unified framework for defining reproducible synovial phenotypes. Therefore, conventional histology and immunohistochemistry still provide a robust and clinically accessible approach to capture biologically meaningful inflammatory patterns in OA, which may serve as a foundation for future integrative studies combining morphology, molecular profiling, and clinical phenotyping.

Several limitations of our study must be acknowledged. First and most importantly, the cohort represents a clinically enriched sample rather than an unselected surgical population. Synovial specimens were submitted for pathological examination at the discretion of the orthopedic surgeon, typically in the presence of overt synovitis or unusual intraoperative findings. As a result, patients with minimal inflammatory features may be underrepresented, potentially inflating the prevalence of high-grade Krenn scores and lympho-myeloid or diffuse-myeloid pathotypes relative to the general OA surgical population. In addition, as a tertiary referral center, our institution may preferentially manage more complex OA cases, which could further contribute to an enrichment of inflammatory and structurally advanced phenotypes. Therefore, while the dataset offers a detailed and biologically informative view of inflammatory phenotypes in advanced OA, generalizability to routine arthroplasty cohorts or early-stage disease should be interpreted cautiously.

Second, although the overall sample size is relatively large, the number of specimens from joints other than the hip and knee is small, limiting the power of joint-specific analyses for these anatomical sites. Third, postoperative pain and late complication data were not available for all patients, which may introduce response bias, although missingness was moderate. Additionally, the categorization of synovial pathotypes

relies on semi-quantitative scoring, which, although validated and reproducible, may miss subtle transcriptomic or cellular heterogeneity detectable through high-dimensional techniques such as spatial transcriptomics or single-cell profiling (53–55).

CONCLUSIONS

Overall, despite these constraints, the study provides a histologically detailed assessment of OA synovium across multiple joints, reinforcing the concept that OA is not merely a degenerative condition, but a heterogeneous inflammatory disease with immunopathologic features shared with RA. In a large, well-phenotyped surgical cohort, we characterized three reproducible synovial pathotypes using an established classification, with the lympho-myeloid form accounting for over half of all specimens and showing the highest levels of systemic inflammatory markers. Despite variation in immune cell composition across joints, histological synovitis was consistently prevalent. Synovial pathotypes were not redundant with conventional histological grading and showed no association with short-term surgical outcomes. These findings support the potential biological relevance of synovial inflammation in OA and suggest that tissue-based profiling may help inform future strategies for patient stratification and targeted therapy development.

LIST OF ABBREVIATIONS

- **BMI**: Body mass index
- **CCI**: Charlson Comorbidity Index
- **CE-AVEC**: Comitato Etico Area Vasta Emilia Centro
- **CI**: Confidence interval
- **CRP**: C-reactive protein
- **DAB**: Diaminobenzidine
- **DAMPs**: Damage-associated molecular patterns
- **EDTA**: Ethylenediaminetetraacetic acid
- **EU GDPR**: European Union General Data Protection Regulation
- **GVIF**: Generalized variance inflation factor
- **H&E**: Hematoxylin and eosin
- **IOR**: Istituto Ortopedico Rizzoli
- **IQR**: Interquartile range
- **KL**: Kellgren–Lawrence
- **MLR**: Monocyte-to-lymphocyte ratio
- **MRI**: Magnetic resonance imaging
- **NLR**: Neutrophil-to-lymphocyte ratio
- **NRS**: Numerical rating scale
- **OA**: Osteoarthritis
- **OR**: Odds ratio
- **PLR**: Platelet-to-lymphocyte ratio
- **RA**: Rheumatoid arthritis
- **REDCap**: Research Electronic Data Capture
- **SII**: Systemic immune-inflammation index
- **Tris-EDTA**: Tris–ethylenediamine tetraacetic acid

DECLARATIONS

ETHICS APPROVAL AND CONSENT TO PARTICIPATE

The study was conducted in accordance with the Declaration of Helsinki. The protocol was approved by the Area Vasta Emilia Centro Ethics Committee (Comitato Etico AVEC) (CE-AVEC 732/2024/Sper/IOR). Written informed consent was obtained from all reachable participants. For patients who could not be contacted, the requirement for informed consent was waived by the Ethics Committee.

CONSENT FOR PUBLICATION

Not applicable.

AVAILABILITY OF DATA AND MATERIALS

The datasets generated and/or analysed during the current study are not publicly available due to institutional and privacy restrictions but are available from the corresponding author on reasonable request.

COMPETING INTERESTS

The authors declare that they have no competing interests.

FUNDING

The authors received no specific funding for this work.

AUTHORS' CONTRIBUTIONS

JC and FU contributed to the conception and design of the study. JC, LB, MG, AR, and DG were involved in the collection and assembly of data. MG, AR, CF, and SZ contributed to the provision of study materials. MG and AR performed the histological and immunohistochemical assessment. JC, DG, RC, TWJH, and FU contributed to the analysis and interpretation of the data. JC and FU provided statistical expertise. JC and LB drafted the article. All authors critically revised the article for important intellectual content and approved the final version. JC and FU act as guarantors and take responsibility for the integrity of the work as a whole.

ACKNOWLEDGEMENTS

Not applicable.

REFERENCES

1. Poole AR. Osteoarthritis as a whole joint disease. HSS J. 2012 Feb;8(1):4–6. doi:10.1007/s11420-011-9248-6 PubMed PMID: 23372516; PubMed Central PMCID: PMC3295952.

2. Martel-Pelletier J, Barr AJ, Cicuttini FM, Conaghan PG, Cooper C, Goldring MB, et al. Osteoarthritis. Nat Rev Dis Primers. 2016 Oct 13;2(1):16072. doi:10.1038/nrdp.2016.72

3. Dell'Isola A, Allan R, Smith SL, Marreiros SSP, Steultjens M. Identification of clinical phenotypes in knee osteoarthritis: a systematic review of the literature. BMC Musculoskelet Disord. 2016 Dec;17(1):425. doi:10.1186/s12891-016-1286-2

4. Sanchez-Lopez E, Coras R, Torres A, Lane NE, Guma M. Synovial inflammation in osteoarthritis progression. Nat Rev Rheumatol. 2022 May;18(5):258–75. doi:10.1038/s41584-022-00749-9

5. Aso K, Shahtaheri SM, Hill R, Wilson D, McWilliams DF, Nwosu LN, et al. Contribution of nerves within osteochondral channels to osteoarthritis knee pain in humans and rats. Osteoarthritis and Cartilage. 2020 Sep;28(9):1245–54. doi:10.1016/j.joca.2020.05.010

6. Walsh DA, Bonnet CS, Turner EL, Wilson D, Situ M, McWilliams DF. Angiogenesis in the synovium and at the osteochondral junction in osteoarthritis. Osteoarthritis and Cartilage. 2007 Jul;15(7):743–51. doi:10.1016/j.joca.2007.01.020

7. Lambert C, Zappia J, Sanchez C, Florin A, Dubuc JE, Henrotin Y. The Damage-Associated Molecular Patterns (DAMPs) as Potential Targets to Treat Osteoarthritis: Perspectives From a Review of the Literature. Front Med. 2021 Jan 18;7:607186. doi:10.3389/fmed.2020.607186

8. Millerand M, Berenbaum F, Jacques C. Danger signals and inflammaging in osteoarthritis. Clin Exp Rheumatol. 2019;37 Suppl 120(5):48–56. PubMed PMID: 31621566.

9. Shakoor D, Demehri S, Roemer FW, Loeuille D, Felson DT, Guermazi A. Are contrast-enhanced and non-contrast MRI findings reflecting synovial inflammation in knee osteoarthritis: a meta-analysis of observational studies. Osteoarthritis and Cartilage. 2020 Feb;28(2):126–36. doi:10.1016/j.joca.2019.10.008

10. De Lange-Brokaar BJE, Ioan-Facsinay A, Yusuf E, Kroon HM, Zuurmond AM, Stojanovic-Susulic V, et al. Evolution of synovitis in osteoarthritic knees and its association with clinical features. Osteoarthritis and Cartilage. 2016 Nov;24(11):1867–74. doi:10.1016/j.joca.2016.05.021

11. Guermazi A, Hayashi D, Roemer FW, Zhu Y, Niu J, Crema MD, et al. Synovitis in knee osteoarthritis assessed by contrast-enhanced magnetic resonance imaging (MRI) is associated with radiographic tibiofemoral osteoarthritis and MRI-detected widespread cartilage damage: the MOST study. J Rheumatol. 2014 Mar;41(3):501–8. doi:10.3899/jrheum.130541 PubMed PMID: 24429179; PubMed Central PMCID: PMC5476295.

12. Mathiessen A, Conaghan PG. Synovitis in osteoarthritis: current understanding with therapeutic implications. Arthritis Res Ther. 2017 Dec;19(1):18. doi:10.1186/s13075-017-1229-9

13. Najm A, Orr C, Gallagher L, Biniecka M, Gaigneux E, Le Goff B, et al. Knee joint synovitis: study of correlations and diagnostic performances of ultrasonography compared with histopathology. RMD Open. 2018 Feb;4(1):e000616. doi:10.1136/rmdopen-2017-000616

14. Daghestani HN, Kraus VB. Inflammatory biomarkers in osteoarthritis. Osteoarthritis Cartilage. 2015 Nov;23(11):1890–6. doi:10.1016/j.joca.2015.02.009 PubMed PMID: 26521734; PubMed Central PMCID: PMC4630669.

15. Jin X, Beguerie JR, Zhang W, Blizzard L, Otahal P, Jones G, et al. Circulating C reactive protein in osteoarthritis: a systematic review and meta-analysis. Annals of the Rheumatic Diseases. 2015 Apr;74(4):703–10. doi:10.1136/annrheumdis-2013-204494

16. Pearle AD, Scanzello CR, George S, Mandl LA, DiCarlo EF, Peterson M, et al. Elevated high-sensitivity C-reactive protein levels are associated with local inflammatory findings in patients with osteoarthritis. Osteoarthritis and Cartilage. 2007 May;15(5):516–23. doi:10.1016/j.joca.2006.10.010

17. Slansky E, Li J, Häupl T, Morawietz L, Krenn V, Pessler F. Quantitative determination of the diagnostic accuracy of the synovitis score and its components. Histopathology. 2010 Sep;57(3):436–43. doi:10.1111/j.1365-2559.2010.03641.x

18. Krenn V, Morawietz L, Burmester G, Kinne RW, Mueller-Ladner U, Muller B, et al. Synovitis score: discrimination between chronic low-grade and high-grade synovitis. Histopathology. 2006 Oct;49(4):358–64. doi:10.1111/j.1365-2559.2006.02508.x

19. Nerviani A, Di Cicco M, Mahto A, Lliso-Ribera G, Rivellese F, Thorborn G, et al. A Pauci-Immune Synovial Pathotype Predicts Inadequate Response to TNFα-Blockade in Rheumatoid Arthritis Patients. Front Immunol. 2020 May 5;11:845. doi:10.3389/fimmu.2020.00845

20. Pitzalis C, Kelly S, Humby F. New learnings on the pathophysiology of RA from synovial biopsies. Current Opinion in Rheumatology. 2013 May;25(3):334–44. doi:10.1097/BOR.0b013e32835fd8eb

21. Humby F, Lewis M, Ramamoorthi N, Hackney JA, Barnes MR, Bombardieri M, et al. Synovial cellular and molecular signatures stratify clinical response to csDMARD therapy and predict radiographic progression in early rheumatoid arthritis patients. Annals of the Rheumatic Diseases. 2019 Jun;78(6):761–72. doi:10.1136/annrheumdis-2018-214539

22. Boutet MA, Nerviani A, Fossati-Jimack L, Hands-Greenwood R, Ahmed M, Rivellese F, et al. Comparative analysis of late-stage rheumatoid arthritis and osteoarthritis reveals shared histopathological features. Osteoarthritis and Cartilage. 2024 Feb;32(2):166–76. doi:10.1016/j.joca.2023.10.009

23. Bianchi E, Najm A, Vanbelle S, Le Goff B, Mutijima E, Kaiser MJ, et al. Impact of the biopsy forceps size on histological analysis and performances of the histological scoring systems. Sci Rep. 2022 Apr 5;12(1):5692. doi:10.1038/s41598-022-09704-w

24. Charlson ME, Pompei P, Ales KL, MacKenzie CR. A new method of classifying prognostic comorbidity in longitudinal studies: Development and validation. Journal of Chronic Diseases. 1987 Jan;40(5):373–83. doi:10.1016/0021-9681(87)90171-8

25. Chen XJ, Liao SF, Ouyang QY, Wang P, Huang GL, Zeng SY, et al. Association between systemic Immune-inflammation index, systemic inflammation response index and adult osteoarthritis: national health and nutrition examination survey. BMC Musculoskelet Disord. 2025 May 29;26(1):529. doi:10.1186/s12891-025-08792-9

26. Shi J, Zhao W, Ying H, Du J, Chen J, Chen S, et al. The relationship of platelet to lymphocyte ratio and neutrophil to monocyte ratio to radiographic grades of knee osteoarthritis. Z Rheumatol. 2018 Aug;77(6):533–7. doi:10.1007/s00393-017-0348-7

27. Kellgren JH, Lawrence JS. Radiological Assessment of Osteo-Arthrosis. Annals of the Rheumatic Diseases. 1957 Dec 1;16(4):494–502. doi:10.1136/ard.16.4.494

28. General Assembly of the World Medical Association. World Medical Association Declaration of Helsinki: ethical principles for medical research involving human subjects. J Am Coll Dent. 2014;81(3):14–8. PubMed PMID: 25951678.

29. Knights AJ, Redding SJ, Maerz T. Inflammation in osteoarthritis: the latest progress and ongoing challenges. Current Opinion in Rheumatology. 2023 Mar;35(2):128–34. doi:10.1097/BOR.0000000000000923

30. Sellam J, Berenbaum F. The role of synovitis in pathophysiology and clinical symptoms of osteoarthritis. Nat Rev Rheumatol. 2010 Nov;6(11):625–35. doi:10.1038/nrrheum.2010.159

31. Scanzello CR, McKeon B, Swaim BH, DiCarlo E, Asomugha EU, Kanda V, et al. Synovial inflammation in patients undergoing arthroscopic meniscectomy: Molecular characterization and relationship to symptoms. Arthritis & Rheumatism. 2011 Feb;63(2):391–400. doi:10.1002/art.30137

32. Benito MJ, Veale DJ, FitzGerald O, Van Den Berg WB, Bresnihan B. Synovial tissue inflammation in early and late osteoarthritis. Annals of the Rheumatic Diseases. 2005 Sep;64(9):1263–7. doi:10.1136/ard.2004.025270

33. Krasnokutsky S, Belitskaya-Lévy I, Bencardino J, Samuels J, Attur M, Regatte R, et al. Quantitative magnetic resonance imaging evidence of synovial proliferation is associated with radiographic severity of knee osteoarthritis: Quantitative MRI Evidence and Radiographic Severity of Knee OA. Arthritis & Rheumatism. 2011 Oct;63(10):2983–91. doi:10.1002/art.30471

34. De Lange-Brokaar BJE, Ioan-Facsinay A, Van Osch GJVM, Zuurmond AM, Schoones J, Toes REM, et al. Synovial inflammation, immune cells and their cytokines in osteoarthritis: a review. Osteoarthritis and Cartilage. 2012 Dec;20(12):1484–99. doi:10.1016/j.joca.2012.08.027

35. Ayral X, Pickering EH, Woodworth TG, Mackillop N, Dougados M. Synovitis: a potential predictive factor of structural progression of medial tibiofemoral knee osteoarthritis – results of a 1 year longitudinal arthroscopic study in 422 patients. Osteoarthritis and Cartilage. 2005 May;13(5):361–7. doi:10.1016/j.joca.2005.01.005

36. Rubortone P, De Lorenzis E, Leone F, Tolusso B, Bruno D, Gessi M, et al. Histological synovitis and radiographic damage in knee osteoarthritis: insights from a comprehensive analysis of ultrasound-guided synovial biopsies in 161 patients. RMD Open. 2025 Jul;11(3):e006011. doi:10.1136/rmdopen-2025-006011

37. Cinar I. Histopathological evaluation of synovial tissue in advanced osteoarthritis: A retrospective study based on total knee arthroplasty specimens. Medicine. 2025 Aug 29;104(35):e44152. doi:10.1097/MD.0000000000044152

38. Mussawy H, Zustin J, Luebke AM, Strahl A, Krenn V, Rüther W, et al. The histopathological synovitis score is influenced by biopsy location in patients with knee osteoarthritis. Arch Orthop Trauma Surg. 2021 Apr 10;142(11):2991–7. doi:10.1007/s00402-021-03889-x

39. Wyatt LA, Moreton BJ, Mapp PI, Wilson D, Hill R, Ferguson E, et al. Histopathological subgroups in knee osteoarthritis. Osteoarthritis and Cartilage. 2017 Jan;25(1):14–22. doi:10.1016/j.joca.2016.09.021

40. Perera J, Delrosso CA, Nerviani A, Pitzalis C. Clinical Phenotypes, Serological Biomarkers, and Synovial Features Defining Seropositive and Seronegative Rheumatoid Arthritis: A Literature Review. Cells. 2024 Apr 24;13(9):743. doi:10.3390/cells13090743

41. Lliso-Ribera G, Humby F, Lewis M, Nerviani A, Mauro D, Rivellese F, et al. Synovial tissue signatures enhance clinical classification and prognostic/treatment response algorithms in early inflammatory arthritis and predict requirement for subsequent biological therapy: results from the pathobiology of early arthritis cohort (PEAC). Annals of the Rheumatic Diseases. 2019 Dec;78(12):1642–52. doi:10.1136/annrheumdis-2019-215751

42. Maarseveen TD, Maurits MP, Coletto LA, Perniola S, Böhringer S, Steinz N, et al. Location and amount of joint involvement differentiates rheumatoid arthritis into different clinical subsets. npj Digit Med. 2025 Oct 23;8(1):623. doi:10.1038/s41746-025-01997-1

43. Chow YY, Chin KY. The Role of Inflammation in the Pathogenesis of Osteoarthritis. Mediators Inflamm. 2020;2020:8293921. doi:10.1155/2020/8293921 PubMed PMID: 32189997; PubMed Central PMCID: PMC7072120.

44. Kugler M, Dellinger M, Kartnig F, Müller L, Preglej T, Heinz LX, et al. Cytokine-directed cellular cross-talk imprints synovial pathotypes in rheumatoid arthritis. Annals of the Rheumatic Diseases. 2023 Sep;82(9):1142–52. doi:10.1136/ard-2022-223396

45. Griffin TM, Scanzello CR. Innate inflammation and synovial macrophages in osteoarthritis pathophysiology. Clin Exp Rheumatol. 2019;37 Suppl 120(5):57–63. PubMed PMID: 31621560; PubMed Central PMCID: PMC6842324.

46. Azamar-Llamas D, Hernández-Molina G, Ramos-Ávalos B, Furuzawa-Carballeda J. Adipokine Contribution to the Pathogenesis of Osteoarthritis. Mediators of Inflammation. 2017;2017:1–26. doi:10.1155/2017/5468023

47. Weyand CM, Fulbright JW, Goronzy JJ. Immunosenescence, autoimmunity, and rheumatoid arthritis. Exp Gerontol. 2003 Aug;38(8):833–41. doi:10.1016/s0531-5565(03)00090-1 PubMed PMID: 12915205.

48. Al Sawy ER, Saber MM, Nassar NN, Sayed NSE. Targeting TREM-1 receptors with metformin and pravastatin modulate monosodium iodoacetate-induced osteoarthritis. Inflammopharmacology. 2025 May;33(5):2737–48. doi:10.1007/s10787-025-01738-6 PubMed PMID: 40319222; PubMed Central PMCID: PMC12176996.

49. Maarouf OH, Uehara M, Kasinath V, Solhjou Z, Banouni N, Bahmani B, et al. Repetitive ischemic injuries to the kidneys result in lymph node fibrosis and impaired healing. JCI Insight. 2018 Jul 12;3(13):e120546, 120546. doi:10.1172/jci.insight.120546 PubMed PMID: 29997302; PubMed Central PMCID: PMC6124521.

50. Zhang F, Jonsson AH, Nathan A, Millard N, Curtis M, Xiao Q, et al. Deconstruction of rheumatoid arthritis synovium defines inflammatory subtypes. Nature. 2023 Nov 16;623(7987):616–24. doi:10.1038/s41586-023-06708-y

51. Raut RD, Chakraborty AK, Neogi T, Albro M, Snyder B, Schaer TP, et al. A multi-tissue human knee single-cell atlas identifies that osteoarthritis reduces regenerative tissue stem cells while increasing inflammatory pain macrophages. Commun Biol. 2025 Aug 2;8(1):1146. doi:10.1038/s42003-025-08586-8

52. Delgado-Sanchez I, Fernandez-Pozo N, Duran I. Standardizing single-cell approaches to osteoarthritis: Toward a comprehensive cellular atlas. Osteoarthritis and Cartilage. 2026 Mar;34(3):380–3. doi:10.1016/j.joca.2025.08.016

53. Stephenson W, Donlin LT, Butler A, Rozo C, Bracken B, Rashidfarrokhi A, et al. Single-cell RNA-seq of rheumatoid arthritis synovial tissue using low-cost microfluidic instrumentation. Nat Commun. 2018 Feb 23;9(1):791. doi:10.1038/s41467-017-02659-x

54. Zhang F, Wei K, Slowikowski K, Fonseka CY, Rao DA, Kelly S, et al. Defining inflammatory cell states in rheumatoid arthritis joint synovial tissues by integrating single-cell transcriptomics and mass cytometry. Nat Immunol. 2019 Jul;20(7):928–42. doi:10.1038/s41590-019-0378-1 PubMed PMID: 31061532; PubMed Central PMCID: PMC6602051.

55. Croft AP, Campos J, Jansen K, Turner JD, Marshall J, Attar M, et al. Distinct fibroblast subsets drive inflammation and damage in arthritis. Nature. 2019 Jun 13;570(7760):246–51. doi:10.1038/s41586-019-1263-7